Reconciling depressed Ca^{2+} sparks occurrence with enhanced RyR2 activity in failing mice cardiomyocytes

Gema Ruiz-Hurtado,[1,2,3]* Linwei Li,[1,2]* María Fernández-Velasco,[4] Angélica Rueda,[5] Florence Lefebvre,[1,2] Yueyi Wang,[1,2] Philippe Mateo,[1,2] Cécile Cassan,[6] Barnabas Gellen,[7,8] Jean Pierre Benitah,[1,2] and Ana María Gómez[1,2]

[1]Institut National de la Santé et de la Recherche Médicale (INSERM), UMR-S 1180, LabEx LERMIT, DHU TORINO, and [2]Faculté de Pharmacie, Université Paris Sud, Université Paris-Saclay, 92296 Châtenay-Malabry, France
[3]Instituto de Investigación, Hospital 12 de Octubre, 28041 Madrid, Spain
[4]Instituto de Investigación Hospital Universitario La Paz, 28046 Madrid, Spain
[5]Departamento de Bioquímica, Centro de Investigación y de Estudios Avanzados del IPN, 07360 México City, D.F., México
[6]Maladies infectieuses et vecteurs: écologie, génétique, évolution et contrôle, Institut de recherche pour le développement, 34394 Montpellier, France
[7]INSERM U955 and [8]Department of Cardiology, AP-HP, Henri Mondor Hospital, Université Paris-Est Créteil, 94010 Créteil, France

Abnormalities in cardiomyocyte Ca^{2+} handling contribute to impaired contractile function in heart failure (HF). Experiments on single ryanodine receptors (RyRs) incorporated into lipid bilayers have indicated that RyRs from failing hearts are more active than those from healthy hearts. Here, we analyzed spontaneous Ca^{2+} sparks (brief, localized increased in $[Ca^{2+}]_i$) to evaluate RyR cluster activity in situ in a mouse post-myocardial infarction (PMI) model of HF. The cardiac ejection fraction of PMI mice was reduced to ∼30% of that of sham-operated (sham) mice, and their cardiomyocytes were hypertrophied. The $[Ca^{2+}]_i$ transient amplitude and sarcoplasmic reticulum (SR) Ca^{2+} load were decreased in intact PMI cardiomyocytes compared with those from sham mice, and spontaneous Ca^{2+} sparks were less frequent, whereas the fractional release and the frequency of Ca^{2+} waves were both increased, suggesting higher RyR activity. In permeabilized cardiomyocytes, in which the internal solution can be controlled, Ca^{2+} sparks were more frequent in PMI cells (under conditions of similar SR Ca^{2+} load), confirming the enhanced RyR activity. However, in intact cells from PMI mice, the Ca^{2+} sparks frequency normalized by the SR Ca^{2+} load in that cell were reduced compared with those in sham mice, indicating that the cytosolic environment in intact cells contributes to the decrease in Ca^{2+} spark frequency. Indeed, using an internal "failing solution" with less ATP (as found in HF), we observed a dramatic decrease in Ca^{2+} spark frequency in permeabilized PMI and sham myocytes. In conclusion, our data show that, even if isolated RyR channels show more activity in HF, concomitant alterations in intracellular media composition and SR Ca^{2+} load may mask these effects at the Ca^{2+} spark level in intact cells. Nonetheless, in this scenario, the probability of arrhythmogenic Ca^{2+} waves is enhanced, and they play a potential role in the increase in arrhythmia events in HF patients.

The Journal of General Physiology

INTRODUCTION

Cardiovascular disease is the leading cause of death in the world (Dahlöf, 2010; Lloyd-Jones, 2010). Heart failure (HF) supports an important percentage of the cardiovascular diseases with serious clinical complications including cardiac arrhythmias, in many cases derived from calcium (Ca^{2+})-handling impairment. Among others, Ca^{2+} is a key factor of electrical activation, ion channel gating, and excitation–contraction (EC) coupling in the cardiac muscle. During cardiac EC coupling, Ca^{2+} influx via sarcolemmal L-type Ca^{2+}channels triggers Ca^{2+} release from the SR by RyRs, increasing the cytosolic Ca^{2+} concentration ($[Ca^{2+}]_i$), which activates myocyte contraction (Fabiato and Fabiato, 1975; Bers, 2002). Cytosolic $[Ca^{2+}]_i$ transient results from spatial and temporal summation of elementary Ca^{2+} events named Ca^{2+} sparks (Cheng et al., 1993). This $[Ca^{2+}]_i$ elevation is transient, because Ca^{2+} is promptly extruded to the extracellular medium by the sodium–calcium exchanger (NCX) and pumped back to the SR by the sarco-endoplasmic reticulum Ca^{2+} ATPase (SERCA), whose activity is controlled by phospholamban (PLB). Other systems participate in regaining diastolic $[Ca^{2+}]_i$ but to a minor degree (Bers, 2002).

*G. Ruiz-Hurtado and L. Li contributed equally to this paper.
Correspondence to Ana María Gómez: ana-maria.gomez@inserm.fr; or Gema Ruiz-Hurtado: gemaruiz@h12o.es

Abbreviations used in this paper: EC, excitation–contraction; FDHM, full duration at half-maximum; FWHM, full width at half-maximum; HF, heart failure; NCX, sodium–calcium exchanger; PLB, phospholamban; PMI, post-myocardial infarction; SERCA, sarco-endoplasmic reticulum Ca^{2+} ATPase.

The Rockefeller University Press $30.00
J. Gen. Physiol. Vol. 146 No. 4 295–306
www.jgp.org/cgi/doi/10.1085/jgp.201511366

A significant decrease in the $[Ca^{2+}]_i$ transient amplitude is a common feature observed in human and animal models of HF and contributes to depressed contractile function (Beuckelmann et al., 1992; Kubo et al., 2001; Piacentino et al., 2003). The global $[Ca^{2+}]_i$ transient depends on several factors: the trigger L-type Ca^{2+} current (I_{CaL}), the amount of Ca^{2+} stored in the SR, and the RyR function. I_{CaL} density has been found unaltered in human (Beuckelmann et al., 1992; Piacentino et al., 2003) and most experimental models of HF (Bénitah et al., 2002). However, a defect in the efficacy of I_{CaL} to release Ca^{2+} has been manifested as a significant reduction in the amount of Ca^{2+} sparks triggered by I_{CaL} (Gómez et al., 1997, 2001). This defect in EC coupling can be related to structural alteration of the remodeled cardiomyocyte, which effectively increases the distance between the L-type Ca^{2+} channels and RyRs, as it was first suggested (Gómez et al., 1997), and lately supported by alteration of T-tubular structure and increase in the orphaned RyRs (Wagner et al., 2012). Concomitantly, the reduction in SR Ca^{2+} load in the failing myocyte is an important determinant for the reduced amplitude of the $[Ca^{2+}]_i$ transient amplitude in systole. This reduction has been ascribed to an impairment in the SR Ca^{2+} uptake, related to depressed SERCA function and expression in HF (Mercadier et al., 1990; Meyer et al., 1995; Gaughan et al., 1999) and increased ratio of PLB/SERCA expression and/or PLB hypophosphorylation (Reiken et al., 2003). The NCX expression has also been found to be increased in many HF models, and although its contribution to unload the SR Ca^{2+} is unclear (Bénitah et al., 2002; Gómez et al., 2002; Piacentino et al., 2003), it may participate to deplete Ca^{2+} stores. The reduction in the SR Ca^{2+} load in HF could also be caused by an increase in the Ca^{2+} leak during diastole (Fischer et al., 2013), which has been related to an increase in the RyR phosphorylation status by PKA (Marx et al., 2000; Reiken et al., 2003) or Ca^{2+}/calmodulin-dependent protein kinase II (Ai et al., 2005).

Diastolic Ca^{2+} leak occurs in several forms: as Ca^{2+} sparks, Ca^{2+} waves, or even as image-imperceptible RyR openings (Zima et al., 2010). What remains unclear today is how HF might affect Ca^{2+} spark occurrence in quiescent myocytes. If all other elements of EC coupling were unaffected, enhanced RyR activity might be viewed as an increased occurrence of spontaneous Ca^{2+} sparks. For example, the frequency of Ca^{2+} sparks is greatly enhanced in a pro-arrhythmogenic model caused by RyR point mutation (Fernández-Velasco et al., 2009). In healthy cardiomyocytes, an acute increase in RyR activity only produces transient effects: in a few twitches, the SR Ca^{2+} load is depressed so the $[Ca^{2+}]_i$ transient returns to control values (Trafford et al., 1998). However, in HF, with numerous concomitants alterations, no consensus data have been reported regarding spontaneous Ca^{2+} spark frequency. In fact, the frequency of Ca^{2+} sparks is also dependent on the SR Ca^{2+} load (Györke and Terentyev, 2008). Thus, even if RyRs were more active, this would decrease the SR Ca^{2+} load, depressing RyR activity, until reaching new equilibrium. Moreover, higher activity of RyRs does not exclusively mean more Ca^{2+} sparks. Some authors have reported an increase in the Ca^{2+} spark frequency in HF animal models (Belevych et al., 2011), whereas others demonstrated a significant decrease in the Ca^{2+} spark frequency of isolated cardiomyocytes from patients with terminal HF compared with non-failing individuals (Lindner et al., 2002). But the RyR activity not only depends on its phosphorylation state, but also on its environment, which can be altered in HF. For example, ATP level, which activates the RyR (Laver, 2006), is depressed in HF (Neubauer, 2007). To clarify this point, we hypothesize that the increased activity of RyRs may be masked in intact cardiomyocytes by other alterations, but might be unmasked in permeabilized myocytes where the cytosolic environment is tightly controlled by the used internal solution. Here we show, for the first time, a comparison between Ca^{2+} spark recordings in intact versus permeabilized cardiomyocytes in a mouse model of cardiac dysfunction post-myocardial infarction (PMI).

MATERIALS AND METHODS

All experiments were performed according to the ethical principles laid down by the French Ministry of Agriculture and the European Union Council Directives (2010/63/EU) for the care of laboratory animals.

Induction of myocardial infarction

Myocardial infarction was induced by left coronary artery ligation under anesthesia (2% isoflurane/O_2; AErrane; Baxter) in 16 male C57BL/6J mice (9 wk of age) placed under mechanical ventilation. Left anterior descending coronary artery was visualized and ligated 1–2 mm from the top of the left atrium. A subcutaneous injection of buprenorphine (0.3 mg/ml) was administered for postoperative analgesia. Sham mice ($n = 14$) were subjected to the same surgical procedure but without coronary artery ligation. 4–6 wk after surgery, cardiac contractile function was assessed by M-mode echocardiography. Only PMI hearts that showed a transmural scar greater than four (number of parts occupied by the scar from a total of six, as assessed by visual division of the left ventricle–free wall, as we did before) were used (Perrier et al., 2004).

Echocardiography

Transthoracic echocardiography was performed using a 15-MHz transducer (Vivid 9; GE Healthcare) under 3% isoflurane gas anesthesia. Two-dimensional echocardiography was used to determine left ventricular ejection fraction using a modified version of Simpson's monoplane analysis (Milliez et al., 2009).

Ventricular myocytes isolation

Ventricular myocytes from sham and PMI mice were isolated using an enzymatic perfusion method (Ruiz-Hurtado et al., 2007; Fernández-Velasco et al., 2011). In brief, mice pretreated with 1,000 U/kg heparin were anaesthetized with 50 mg/kg sodium pentobarbital administered intraperitoneally. Hearts were removed and placed in ice-cold oxygenated Tyrode's solution containing (in mmol/liter): 130 NaCl, 0.4 NaH_2PO_4, 5.8 $NaHCO_3$, 0.5 $MgCl_2$, 5.4 KCl, 22 glucose, 25 HEPES, and 10^{-3} insulin, pH 7.4 with NaOH. The aorta was cannulated above the aortic valve and perfused by

gravity at 37°C with preoxygenated Tyrode's solution containing 0.1 mmol/liter EGTA for 2 min. Enzyme solution with 1 g/liter collagenase Type II (Worthington Biochemical Corporation) or 5 g/liter Liberase (TM Research Grade; Roche) in Tyrode's solution supplemented with 0.1 mmol/liter $CaCl_2$ was then perfused until the aortic valve was digested, as assessed by increased efflux. Hearts were removed, cut in small pieces, and gently shaken in enzyme solution supplemented with 2 g/liter BSA for 2 min at 37°C to disperse individual myocytes. Myocytes were then filtered through a 250-µm nylon mesh and centrifuged at 20 *g* for 2 min. A pellet containing myocytes was resuspended in Tyrode's solution supplemented with 0.5 mmol/liter $CaCl_2$ and 2 g/liter BSA, and then centrifuged again. The final pellet was resuspended in storage solution containing Tyrode's solution supplemented with 1 mmol/liter $CaCl_2$.

$[Ca^{2+}]_i$ transients and SR Ca^{2+} load

We used 14 control mice and 16 PMI animals. Isolated ventricular myocytes were loaded with the membrane-permeant Fluo-3 AM, as described previously (Pereira et al., 2012; Ruiz-Hurtado et al., 2012b). Confocal Ca^{2+} images were obtained by exciting the cell at 488 nm, and emission was collected at >505 nm using a laser scanning confocal microscope (LSM510; Carl Zeiss, or SP5; Leica) equipped with a 63× N.A. 1.2 water-immersion objective in the line-scan mode. To record intracellular Ca^{2+} ($[Ca^{2+}]_i$) transients, myocytes were electrically field stimulated by two Pt electrodes at 2 Hz. Before recording, Fluo-3–loaded myocytes were stimulated for 1 min to reach steady state. The fluorescence values (F) were normalized by the basal fluorescence (F_0) to obtain F/F_0. For SR Ca^{2+} load estimation, intact ventricular myocytes were rapidly perfused with 10 mmol/liter caffeine just after field stimulation. The amplitude of caffeine-evoked Ca^{2+} transients was used to assess SR Ca^{2+} load. Fractional SR release was measured by normalizing the steady state of the Ca^{2+} transient (peak F/F_0) by the caffeine-evoked intracellular Ca^{2+} transient (peak F/F_0 evoked by 10 mmol/liter of rapid caffeine application). Post-rest potentiation was calculated by normalizing the first intracellular Ca^{2+} transient (peak F/F_0) after a period of rest from ∼2 min to reach the steady-state $[Ca^{2+}]_i$ transient (Ruiz-Hurtado et al., 2012a).

Ca^{2+} spark recording

To record spontaneous Ca^{2+} sparks and Ca^{2+} waves in intact quiescent cells, after $[Ca^{2+}]_i$ transient recordings, each myocyte was scanned 12 times for 1.5 s at 1.5 ms per line. Ca^{2+} sparks were detected as localized, rapid, and brief elevations in Ca^{2+} fluorescence. Ca^{2+} sparks were detected using an automated detection system (homemade in IDL; Exelis Visual Information Solutions) and a criterion that limited the detection of false events while detecting most Ca^{2+} sparks (Fernández-Velasco et al., 2009). Abnormal spontaneous Ca^{2+} release manifested as Ca^{2+} waves were quantified by the percentage of occurrence. Ca^{2+} wave was identified as an increase in the Ca^{2+} fluorescence starting locally and propagated to one or both sides of the cell (Fernández-Velasco et al., 2009).

In permeabilized myocytes, the basic control internal solution used contained (in mmol/liter): 120 K-aspartate, 10 HEPES, 3 MgATP, 0.5 EGTA, 10 Na phosphocreatine, 5 U/ml creatine phosphokinase, and 0.75 $MgCl_2$, and 8% dextran, pH 7.2. After permeabilization with saponin (0.01% wt/vol for 60 s), this solution was supplemented with 50 µmol/liter K_5-Fluo-3 and enough $CaCl_2$ to reach 50 nmol/liter of free Ca^{2+}, calculated with MAXCHELATOR. Ca^{2+} sparks were recorded after a period of 1 min of stabilization in this internal solution.

In a set of experiments to mimic the pathological conditions of a failing heart, a "failing" internal solution was used, of similar

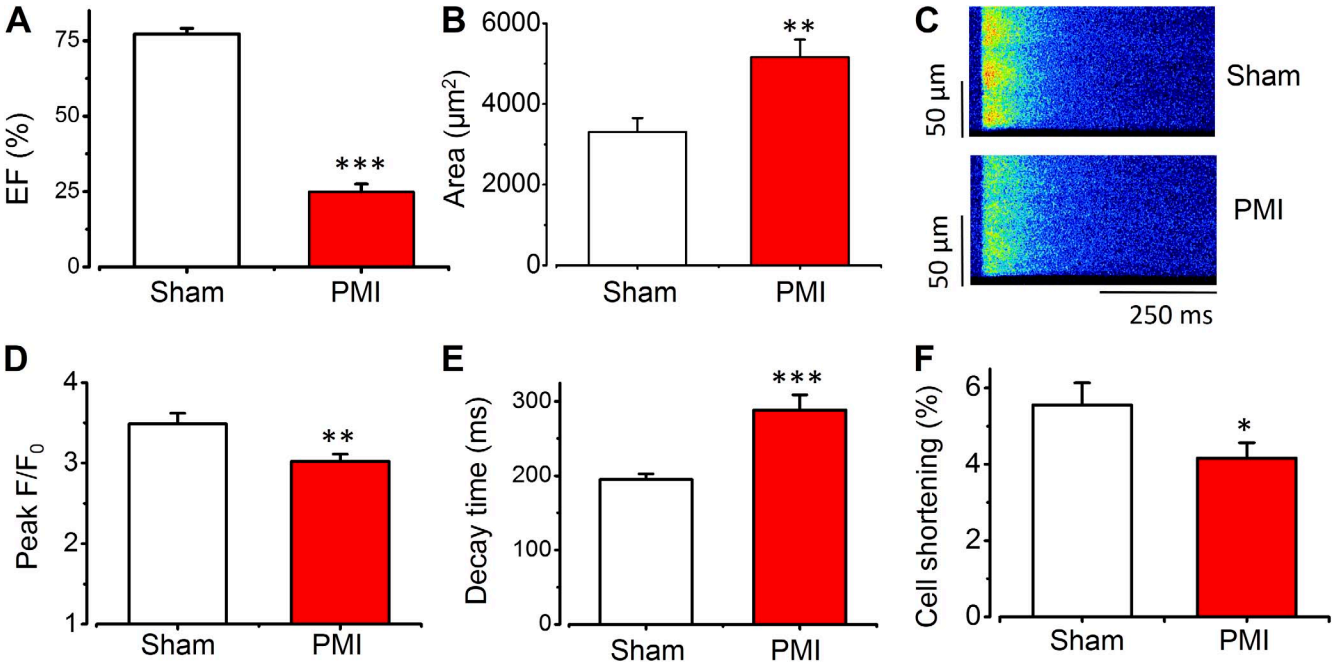

Figure 1. Myocardial infarction induces a decrease in $[Ca^{2+}]_i$ transients. (A) Ejection fraction measured by echocardiography in control (white bar; $n = 12$) and coronary artery occlusion (PMI; red bar; $n = 12$)–operated mice. (B) Cardiomyocyte area expressed in square micrometers for sham (white bar; $n = 14$ cells from three animals) and PMI (red bar; $n = 11$ cells from three animals). (C) Line-scan images during field stimulation at 2 Hz of one ventricular myocyte from sham (top) or PMI (bottom) mice. (D–F) Intracellular $[Ca^{2+}]_i$ transient peak (D), decay time (E), and cell shortening (F; 34 cells from eight sham mice and 30 cells from eight PMI mice) in ventricular myocytes. Peak expressed as maximum F/F_0, where F is the fluorescence trace and F_0 is the fluorescence during the diastolic period. *, $P < 0.05$; **, $P < 0.01$; ***, $P < 0.001$ versus myocytes from sham mice. Error bars represent the SEM.

composition to the basic control solution, but ATP and creatine phosphokinase were reduced by half, and inorganic phosphates were added (6.5 mmol/liter K_2HPO_4) (Ingwall, 2006, 2009). To maintain the total amount of Mg, while reducing MgATP concentrations, the amount of $MgCl_2$ was increased to 2.25 mmol/liter.

SR Ca^{2+} load in permeabilized myocytes was estimated by rapid 20-mmol/liter caffeine application (solved in basic or failing solution) after Ca^{2+} spark recording.

Statistical analyses

Data are presented as means ± SEM. Statistical significance was evaluated by Student's *t* test. For statistical comparison of occurrence, Ca^{2+} waves and triggered activity Gaussian Fisher's χ^2 test was used. Preliminary descriptive analyses included frequencies for categorical variables and mean ± SD for continuous variables. A conditional hierarchical linear model was used (SAS/UNIX statistical software; PROC MIXED; SAS Institute) to compare continuous variables between groups to take into account the multiple observations per animal. The group was a fixed effect, and animals were a random effect nested in the group; in the case of repeated measurements on cells, we added a random effect for cells in animals.

RESULTS

Ca^{2+} release and SR Ca^{2+} load after myocardial infarction

Hearts from PMI mice showed a significant reduction in the ejection fraction, measured by echocardiography, compared with hearts from sham mice (Fig. 1 A). Cellular hypertrophy was assessed by cardiomyocyte area measured by confocal microscopy images of isolated ventricular myocytes. Cardiomyocytes from PMI mice showed significantly higher cellular area than myocytes from sham-operated animals, indicating hypertrophy at the cellular level (Fig. 1 B). To determine whether intracellular Ca^{2+} handling was altered in hypertrophied myocytes from PMI mice, we analyzed $[Ca^{2+}]_i$ transients. Fig. 1 C shows representative line-scan images of evoked $[Ca^{2+}]_i$ transients from sham (top) and PMI (bottom) cardiomyocytes. The $[Ca^{2+}]_i$ transients recorded in PMI myocytes were smaller in amplitude than those recorded in control myocytes. The average amplitude of $[Ca^{2+}]_i$ transients showed a significant reduction in myocytes from PMI mice compared with myocytes from sham-operated mice (Fig. 1 D). $[Ca^{2+}]_i$ transient decay time (Fig. 1 E) was significantly prolonged in myocytes from PMI mice compared with those from sham-operated mice, suggesting slower Ca^{2+} uptake by the SERCA pump. Cellular shortening was also significantly decreased in myocytes from PMI mice (Fig. 1 F). Because SR Ca^{2+} load is determinant in $[Ca^{2+}]_i$ transient amplitude, we measured SR Ca^{2+} content by rapid caffeine application, as

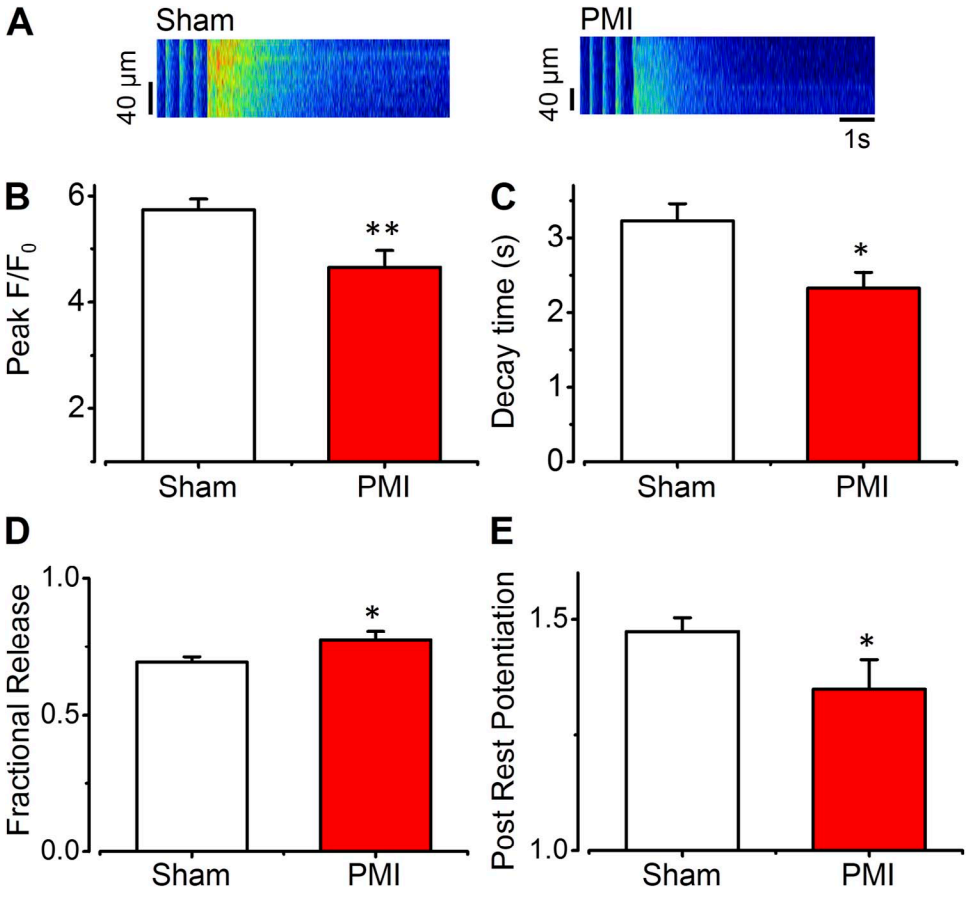

Figure 2. Myocardial infarction induces a decrease in SR Ca^{2+} load. (A) Line-scan images of caffeine-evoked intracellular Ca^{2+} transients after field stimulation at 2 Hz in one ventricular myocyte from sham (left) or PMI (right) mice obtained by the application of 10 mmol/liter caffeine. (B) Averaged caffeine-evoked Ca^{2+} transient peak (F/F_0) of myocytes from sham (white bar; $n = 43$ cells from six animals) and PMI (red bar; $n = 21$ cells from five animals) mice. (C) Averaged decay time constant of the caffeine-evoked Ca^{2+} transient (34 cells from six sham animals; 13 cells from five PMI animals). (D) Fractional SR Ca^{2+} release during field stimulation at 2 Hz in control myocytes (white bar; $n = 36$ cells from three animals) and in cells from PMI mice (red bar; $n = 20$ cells from three animals). (E) Post-rest potentiation (white bar; $n = 36$ cells from three animals) and in cells from PMI mice (red bar; $n = 20$ cells from three animals). Error bars represent the SEM. *, $P < 0.05$; **, $P < 0.001$ PMI versus sham.

exemplified in Fig. 2 for one sham myocyte (left) and one hypertrophied myocyte from PMI mouse (right). The averaged caffeine-evoked $[Ca^{2+}]_i$ transients were smaller in PMI myocytes compared with sham myocytes (Fig. 2 B). Thus, the decrease in $[Ca^{2+}]_i$ transient amplitude might be related, at least in part, to the decrease in SR Ca^{2+} load. Caffeine-evoked $[Ca^{2+}]_i$ transient decay was significantly accelerated in myocytes from PMI mice (Fig. 2 C), suggesting faster Ca^{2+} extrusion through the NCX. We also estimated the fractional release in electrically evoked beats by normalizing $[Ca^{2+}]_i$ transient amplitude by the SR Ca^{2+} load (see Materials and methods). We observed that myocytes from PMI mice showed increased fractional release compared with sham myocytes (Fig. 2 D), suggesting higher RyR activity, even if the $[Ca^{2+}]_i$ transient is depressed. However, the capacity of the SR to accumulate Ca^{2+} during rest, as estimated by the post-rest potentiation, was decreased in PMI cardiomyocytes (Fig. 2 E).

Opposite effect in spark-mediated Ca^{2+} leak in intact versus permeabilized myocytes after myocardial infarction

The increase in fractional release may reflect a higher sensitivity of RyRs to Ca^{2+} in PMI mice. The opening of a RyR cluster induces rapid, local, and brief $[Ca^{2+}]_i$ elevation known as Ca^{2+} spark (Cheng et al., 1993). We therefore recorded Ca^{2+} sparks in quiescent cells, as exemplified in Fig. 3 A in cardiac myocytes from sham (left) and PMI mice (right). Surprisingly, contrary to the supposed increased activity of RyR based on the fractional release data (Fig. 2 D), cardiomyocytes from PMI hearts showed a significant decrease in Ca^{2+} spark frequency (Fig. 3 A, bottom).

However, single-channel data have shown higher activity of RyR in failing hearts (Marx et al., 2000), so an increase in Ca^{2+} sparks was expected. To resolve this discrepancy, we analyzed Ca^{2+} sparks in permeabilized myocytes (Pereira et al., 2006). Under these conditions, sarcolemmal fluxes (NCX, I_{CaL}) are invalidated. Moreover, this maneuver allows us to analyze Ca^{2+} sparks in the same cytoplasmic environment for both cell types (same ATP, Ca^{2+}, Mg concentration). Fig. 3 B illustrates Ca^{2+} spark occurrence in myocytes from the sham mouse (left) and PMI mouse (right). After permeabilization, myocytes from PMI mice did exhibit significantly higher Ca^{2+} spark frequency than control myocytes (Fig. 3 B, bottom).

To asses biophysical characteristics of Ca^{2+} sparks, we analyzed their amplitude (measured as the peak F/F_0), full duration at half-maximum (FDHM), and full width

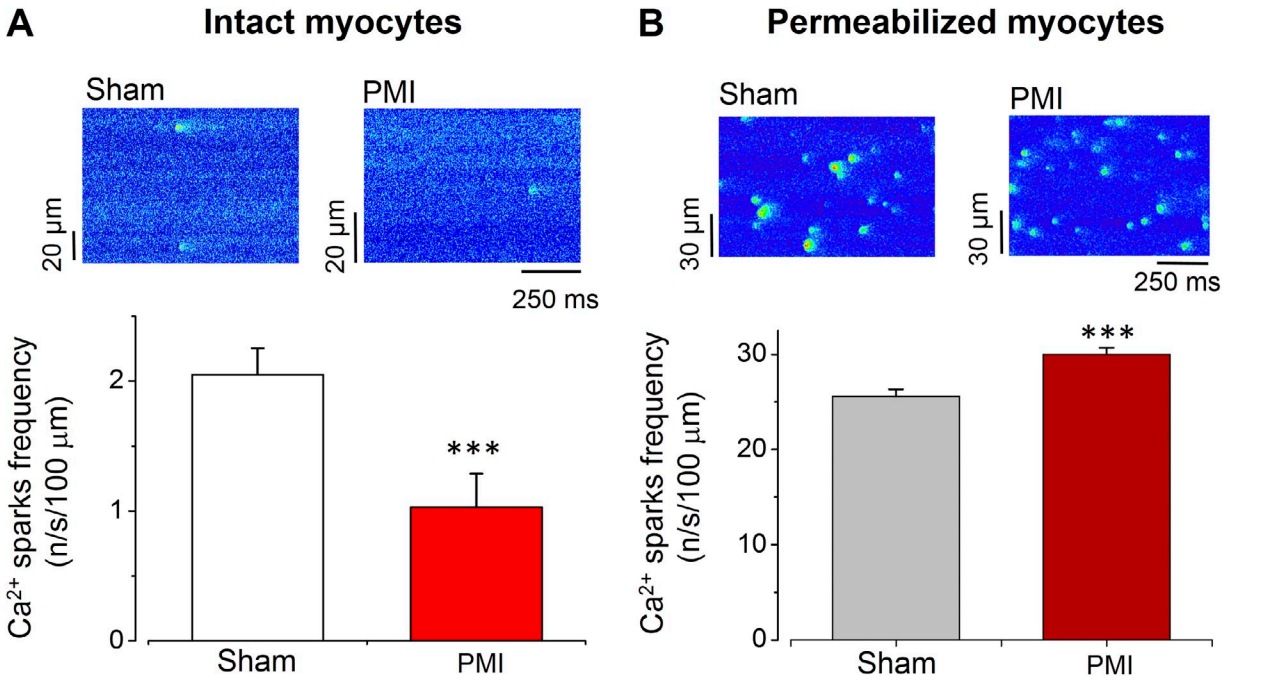

Figure 3. Ca^{2+} spark frequency in intact versus permeabilized myocytes after myocardial infarction. (A; top) Line-scan images obtained in intact myocytes from sham (left) or from PMI (right) mice. (Bottom) Bar graph showing the Ca^{2+} spark frequency in intact cells from sham ($n = 59$ from five animals) and PMI mice ($n = 41$ from seven animals). (B; top) Line-scan images obtained in permeabilized at 50 nmol/liter $[Ca^{2+}]_i$ myocytes from sham (left) or from PMI (right) mice. (Bottom) Bar graph showing the increased Ca^{2+} spark frequency in permeabilized cells from PMI mice ($n = 27$ cells from three animals) compared with myocytes from sham mice ($n = 26$ cells from three animals). ***, $P < 0.001$ versus myocytes from sham mice. Error bars represent the SEM.

at half-maximum (FWHM) in intact and permeabilized myocytes from sham and PMI mice. Fig. 4 A shows that Ca^{2+} spark amplitudes were smaller in intact PMI myocytes than in intact sham myocytes. Duration was also considerably reduced in intact PMI myocytes (Fig. 4 B), whereas no significant change was observed with respect to half-width (Fig. 4 C). A similar trend was observed in Ca^{2+} spark characteristics in permeabilized cardiomyocytes (Fig. 4, D–F), suggesting that alteration in the intrinsic RyR cluster activity or structural organization is behind alterations of Ca^{2+} spark characteristics in HF.

RyR environment in intact cells reduces probability of Ca^{2+} sparks

To investigate the discrepancy between Ca^{2+} spark occurrence in intact versus permeabilized PMI myocytes, we addressed two possible mechanisms. It is well known that the amount of Ca^{2+} stored in the SR influences Ca^{2+} spark frequency (Györke and Terentyev, 2008). We found that the SR Ca^{2+} load is significantly reduced in intact PMI cells (Fig. 2). However, as shown in Fig. 5 A, in permeabilized myocytes, the SR load was not significantly different (P = 0.08) between myocytes isolated from sham or PMI mice, suggesting that the SR Ca^{2+} load depletion contributes to depression of Ca^{2+} spark rate in intact PMI cells. In fact, normalizing in each cell the Ca^{2+} spark occurrence by the amount of Ca^{2+} stored in the SR, we found in permeabilized myocytes that the frequency of Ca^{2+} spark by a given amount of Ca^{2+} stored in the SR is significantly higher in PMI than in sham myocytes (Fig. 5 B), whereas similar analysis in intact cells showed that the Ca^{2+} spark frequency remains decreased in PMI intact myocytes, even after normalizing it to the SR load (Fig. 5 C). This suggested that even if the SR Ca^{2+} load decrease may participate in the reduced Ca^{2+} spark occurrence, other mechanisms might also contribute. As ATP modifies RyR function (Meissner et al., 1986; Laver, 2010; Tencerová et al., 2012), and its levels are known to be decreased in HF (Ingwall, 2006, 2009), we repeated the Ca^{2+} spark measurements in permeabilized cardiomyocytes first with control intracellular media and then with a decreased energetic source media, which mimicked failing status (see Materials and methods). Fig. 6 A shows examples of the same cells from sham (left) and PMI heart (right) in control (top) and "failing" (bottom) solutions, illustrating that Ca^{2+} sparks were reduced in failing solution. On average (Fig. 6 B), the modified internal solution to mimic HF environment significantly reduced Ca^{2+} spark frequency in both sham and

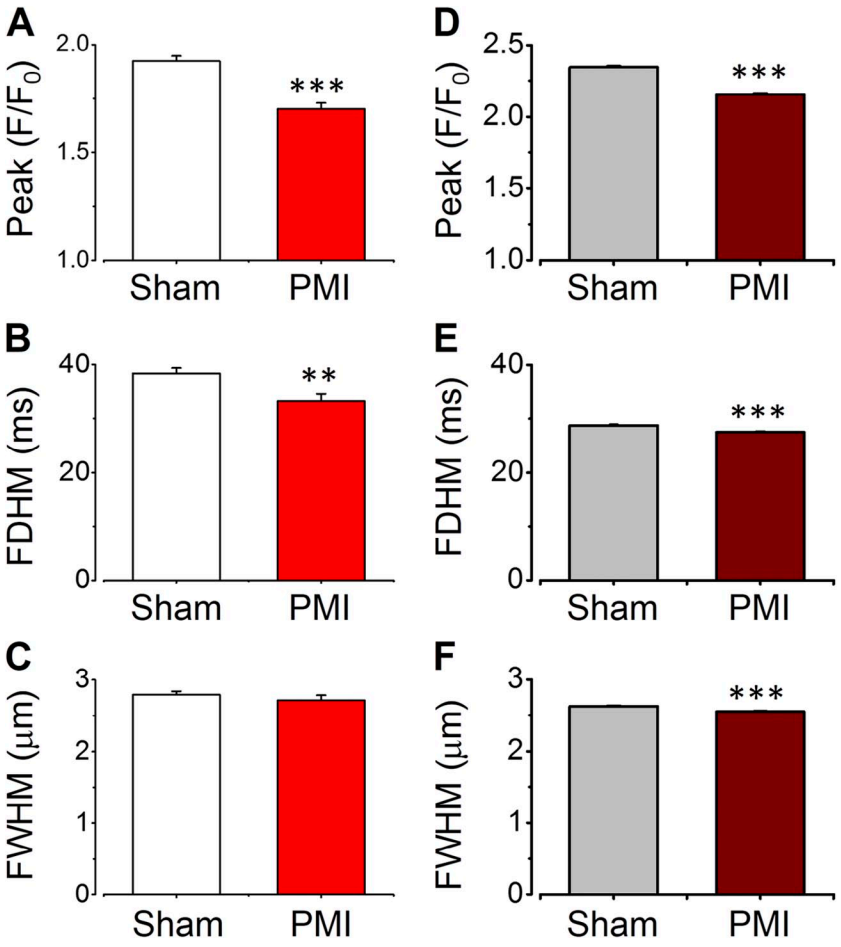

Figure 4. Difference in the Ca^{2+} spark characteristics between intact versus permeabilized myocytes after myocardial infarction. (A–C) Ca^{2+} spark amplitude (A; peak F/F_0), duration at half-peak amplitude (B; FDHM), and width at half-peak amplitude (C; FWHM) in intact myocytes from sham (n = 442 Ca^{2+} sparks, from 22 cells, from three hearts) and PMI mice (n = 160 Ca^{2+} sparks, from 24 cells, from three hearts). (D–F) Same as A–C but in permeabilized myocytes from sham (n = 7,806 Ca^{2+} sparks, from 26 cells, from three hearts) and PMI (n = 9,783 Ca^{2+} sparks, from 27 cells, from three hearts) mice. **, P < 0.01; ***, P < 0.001 versus myocytes from sham mice. Error bars represent the SEM.

PMI myocytes. In this condition, the SR Ca^{2+} load was unchanged between permeabilized cells from sham and PMI heart (Fig. 6 B). In addition, biophysical characteristics of Ca^{2+} sparks, namely amplitude (Fig. 6 C), duration (Fig. 6 D), and spatial spread (Fig. 6 E), remained reduced in PMI cells compared with sham cells in the failing solution.

Ca^{2+} waves and triggered activity after myocardial infarction

To determine whether the depressed Ca^{2+} spark occurrence in intact cells may be protective of the cells from arrhythmia, we checked for Ca^{2+} waves and triggered activity during the rest period after one stimulation train (at 2 Hz) in the absence or presence of β-adrenergic stimulation (1 µmol/liter isoproterenol). Fig. 7 A shows that the occurrence of Ca^{2+} waves was significantly higher in myocytes from PMI mice compared with those from sham-operated mice during the diastolic period. Moreover, myocytes from PMI showed a higher occurrence of triggered activity than myocytes from sham mice, and this effect was enhanced by β-adrenergic stimulation (Fig. 7 B).

DISCUSSION

In this paper, we have analyzed Ca^{2+} sparks in a mouse model of HF after myocardial infarction and demonstrated that even if RyRs showed signs of enhanced activity, Ca^{2+} sparks in intact cardiomyocytes were less frequent in PMI myocytes, although more Ca^{2+} waves were formed. Cell permeabilization unmasked the defect, unveiling enhanced Ca^{2+} spark occurrence in failing cardiomyocytes. The alterations in the SR Ca^{2+} load and cytosolic environment contributed to the depression in Ca^{2+} spark occurrence in intact myocytes from HF mice.

In the model we used herein, the hearts presented big transmural infarctions, ventricular myocytes were hypertrophied, and echocardiography measurements showed a depressed contractile function of the heart

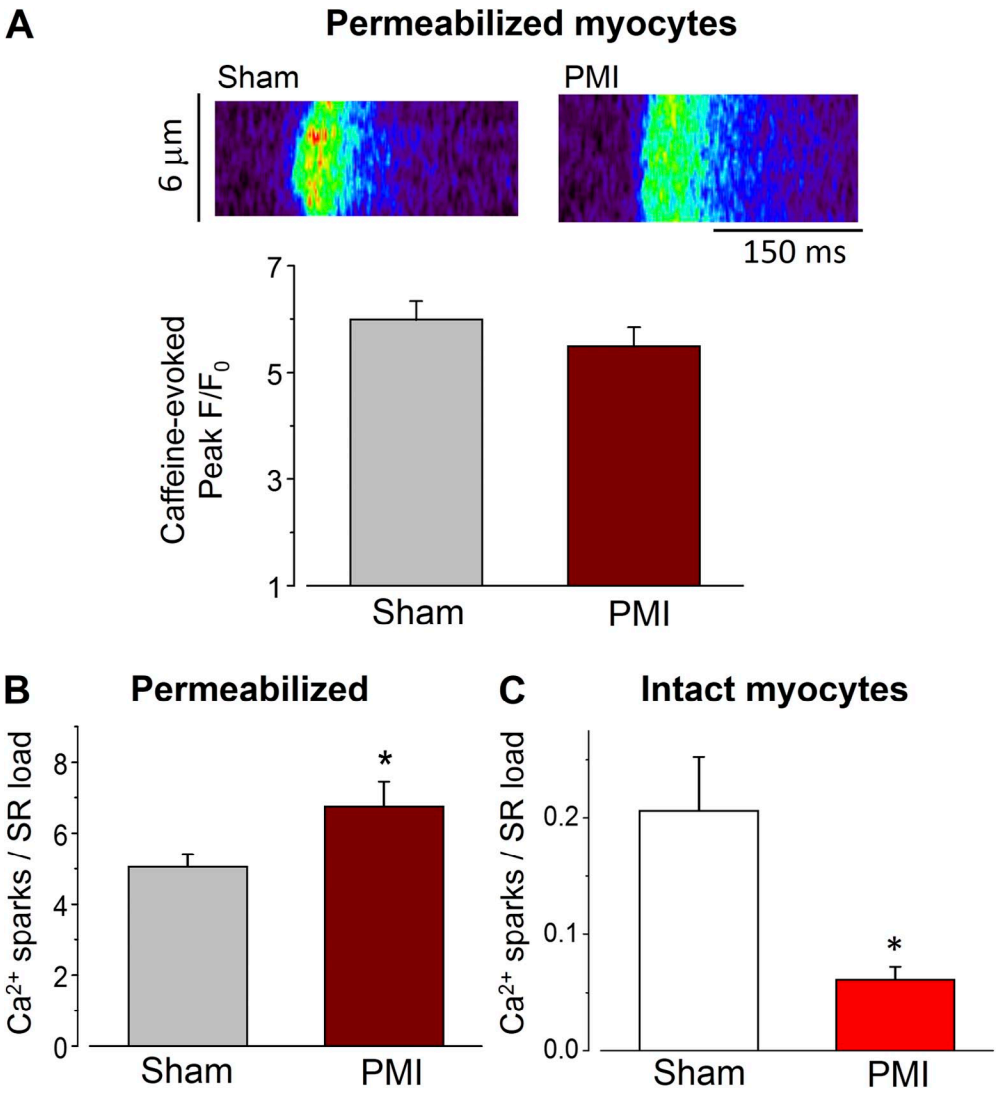

Figure 5. Permeabilized myocytes from PMIs show similar Ca^{2+} load but higher Ca^{2+} sparks per load unit than sham cells. (A; top) Line-scan images of representative caffeine-evoked Ca^{2+} release in permeabilized myocytes from sham (left) or from PMI (right) mice. (Bottom) Caffeine-evoked Ca^{2+} transient peak (F/F_0) of permeabilized myocytes from sham (gray bar; n = 14 cells from three animals) and PMI (dark red bar; n = 15 cells from three animals) mice. (B) Ca^{2+} spark frequency normalized to SR load in permeabilized cells from sham (gray bar; n = 13 from three animals) and PMI mice (dark red bar; n = 12 cells from three animals). (C) Ca^{2+} spark frequency normalized to SR load in intact cells from sham (white bar; n = 10 from four animals) and PMI mice (red bar; n = 9 cells from four animals). *, $P < 0.05$ versus myocytes from sham mice. Error bars represent the SEM.

(Fig. 1). At the cellular level, the amplitude of the $[Ca^{2+}]_i$ transient was reduced, and the decay time prolonged, in agreement with decreased SR Ca^{2+} load (Fig. 2). Interestingly, spontaneous Ca^{2+} sparks recorded during rest period were less frequent in PMI than in control cells (Fig. 3), which is consistent with the depressed SR Ca^{2+} load but inconsistent with the reported higher RyR2 activity (Marx et al., 2000).

Since the first report on Ca^{2+} sparks in an animal model of HF (Gómez et al., 1997), conflicting results have been reported regarding the Ca^{2+} sparks. Although the first study found a decrease in evoked Ca^{2+} sparks in two rat HF models (Gómez et al., 1997), a later one showed an increase (Shorofsky et al., 1999). However, the latter study concerned a model of compensated cardiac hypertrophy, where the cardiac function was normal, thus without signs of HF. The confounding results regarding the occurrence on Ca^{2+} sparks was further complicated by the observation that single RyR channel activity, measured in isolated RyR incorporated into lipid bilayers, showed higher activity in failing hearts (Marx et al., 2000). Ca^{2+} sparks are described as the elementary events of SR Ca^{2+} release through RyRs, which can be visualized using appropriated techniques. Thus, an increase in RyR activity by either PKA (Marx et al., 2000) or calmodulin-dependent protein kinase II (Ai et al., 2005) phosphorylation, FKBP12.6 down-regulation (Marx et al., 2000), or RyR oxidation (Terentyev et al., 2008), among others, should be translated into a higher than normal Ca^{2+} spark frequency. In our experiments, we did not find increased,

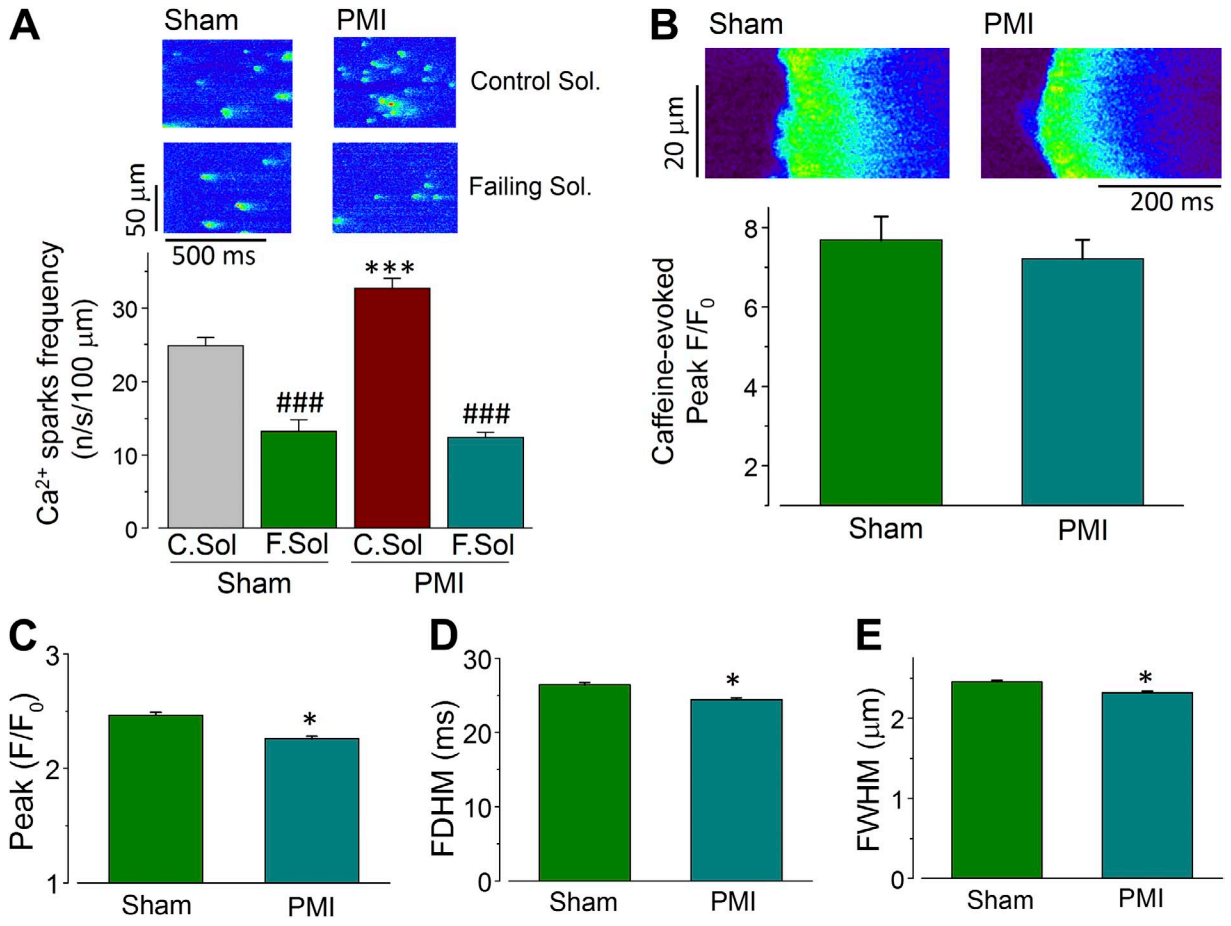

Figure 6. RyR metabolic environment influences Ca^{2+} spark release in PMI mice. (A; top) Representative line-scan images of Ca^{2+} sparks obtained in permeabilized myocytes from sham (left) or from PMI (right) mice, with the same cell first in control (C.Sol.; top) and then "failing" (F.Sol.; bottom) solutions. (Bottom) Bar graph showing the average data of Ca^{2+} spark frequency in permeabilized cells from sham ($n = 6$) and PMI mice ($n = 8$) in control (Ct.Sol.; gray and dark red bars for sham and PMI, respectively) and failing solutions (F.Sol.; dark green for sham and dark cyan bar for PMI). (B; top) Line-scan examples of caffeine-evoked Ca^{2+} release in permeabilized myocytes in failing solution from sham (left) or from PMI (right) mice. (Bottom) Averaged caffeine-evoked Ca^{2+} transient peak (F/F_0) of permeabilized myocytes from sham (dark green bar; $n = 6$ cells from two animals) and PMI (blue bar; $n = 8$ cells from two animals) mice. (C–E) Ca^{2+} spark characteristics, Ca^{2+} spark amplitude (peak F/F_0; C), Ca^{2+} spark duration at half-peak amplitude (FDHM; D), and Ca^{2+} spark width at half-peak amplitude (FWHM; E) of permeabilized myocytes from sham (dark green bar; $n = 1{,}263$ Ca^{2+} sparks, from six cells, from two hearts) and PMI (dark cyan bar; $n = 1{,}391$ sparks, from eight cells, from two hearts) mice in failing solutions. *, $P < 0.05$ versus myocytes from sham mice; ***, $P < 0.001$ versus Sham cells in control solution; ###, $P < 0.001$ versus the same group of myocytes in control solution. Error bars represent the SEM.

but rather decreased, Ca^{2+} spark frequency, which is consistent with the depression in SR Ca^{2+} content (Fig. 2). In fact, Ca^{2+} spark frequency is highly dependent on Ca^{2+} content in the SR (Zima et al., 2010). However, our data did show hints indicating that the RyR is more active in HF cardiomyocytes. In fact, in Fig. 7 we evidenced an enhanced diastolic leak in the form of Ca^{2+} waves in PMI myocytes. This indicates a higher propensity for Ca^{2+} released in a RyR cluster to activate neighboring clusters and propagate throughout the cell in arrhythmogenic Ca^{2+} waves. Thus, diastolic Ca^{2+} release is higher in PMI cells, although Ca^{2+} sparks are not. Moreover, the fractional release (calculated as the amount of Ca^{2+} released in each twitch normalized to the amount of Ca^{2+} stored in the SR) is significantly higher in PMI cells, indicating favored Ca^{2+} release when triggered. Cells from small rodents such as mice accumulate Ca^{2+} inside the SR during resting periods, which depend, among others factors, on the balance between Ca^{2+} leak and SERCA activity. We have measured this property as post-rest potentiation, a measurement of the enhancement of the $[Ca^{2+}]_i$ transient amplitude after a rest period compared with the average $[Ca^{2+}]_i$ transient amplitude in steady state during continued electrical stimulation. We found that the post-rest potentiation is less important in PMI cardiomyocytes, suggesting that the Ca^{2+} leak during rest may be more important. This is not incompatible with the decreased frequency of Ca^{2+} sparks in intact PMI

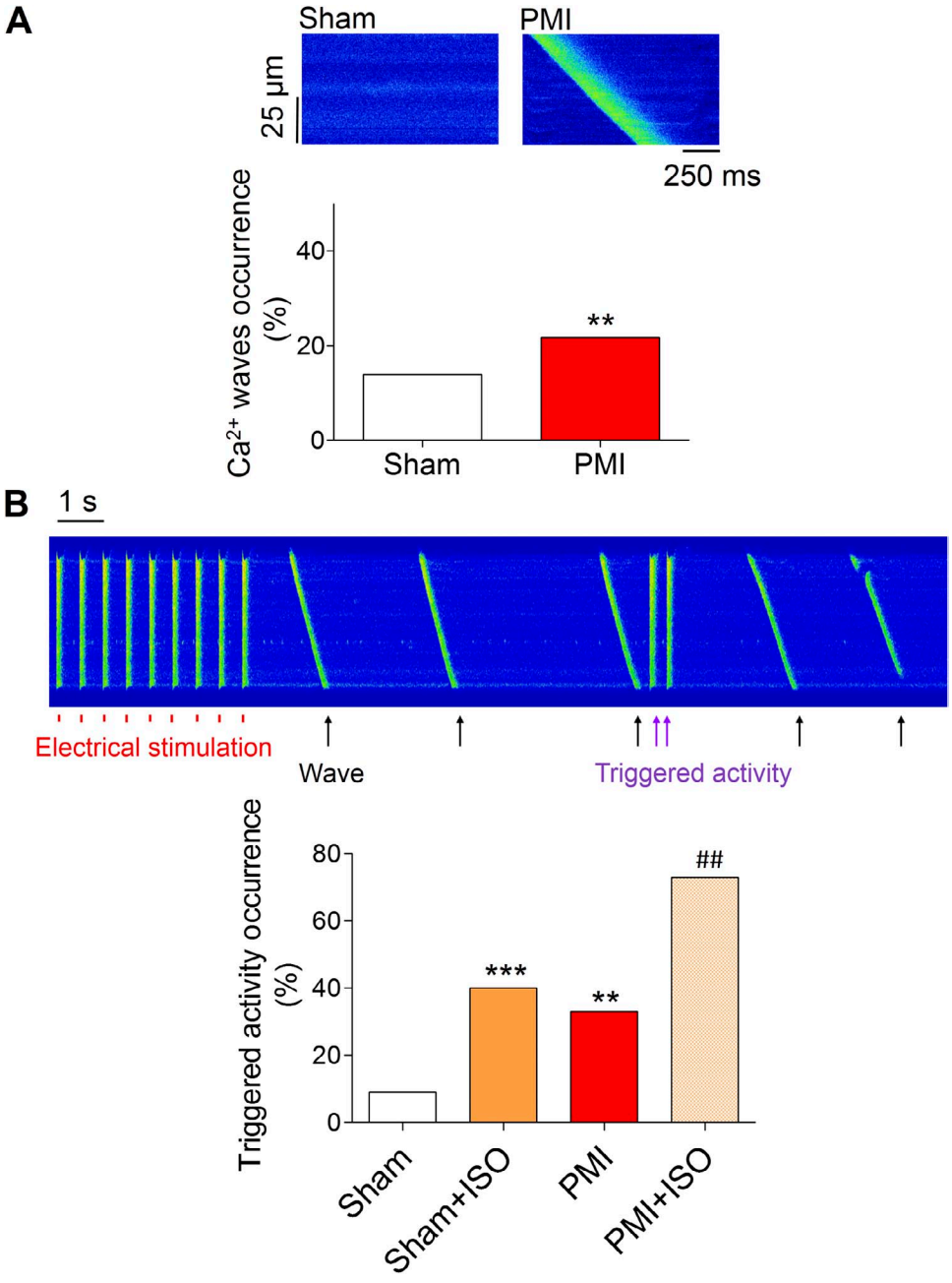

Figure 7. Myocardial infarction induces pro-arrhythmogenic Ca^{2+} release. (A; top) Line-scan images of representative spontaneous Ca^{2+} wave release during diastole (top) in one ventricular myocyte from sham (left) or PMI (right) mice. (Bottom) Occurrence of Ca^{2+} waves expressed as percentage (bottom) in cells from sham mice (white bar; n = 22) and in cells from PMI mice (red bar; n = 24). (B; top) Line-scan image of one ventricular myocyte isolated from PMI mice during electric stimulation at 2 Hz and during isoproterenol application. Red lines indicate electrical stimulation, and violet arrows indicate spontaneous triggered activity during diastole. (Bottom) Occurrence of abnormal triggered activity in myocytes from sham (white bar; n = 10) or PMI (red bar; n = 13) mice, and in myocytes from sham or PMI mice in the presence of 1 µmol/liter isoproterenol (orange bar for sham, n = 10; cross-hatched orange bar for PMI, n = 13). n = 3 hearts per group. **, $P < 0.01$; ***, $P < 0.001$ versus myocytes from sham mice; ##, $P < 0.01$ versus myocytes from PMI mice.

cardiomyocytes. In fact, although Ca^{2+} sparks were first described as the elementary event of Ca^{2+} release through RyRs, nonspark Ca^{2+} release can happen through RyRs (Lipp and Niggli, 1996; Zima et al., 2010), and the dependency of this release on the SR Ca^{2+} load is less steep than that of Ca^{2+} sparks (Lipp and Niggli, 1996). Moreover, PMI cells showed more diastolic Ca^{2+} release measured as Ca^{2+} waves (Fig. 7). Because HF is a complex process, where other Ca^{2+}-handling proteins show altered expression or function, and also the cytosolic environment around the RyR may be altered, an enhanced RyR activity may not be visualized as an elevated occurrence of Ca^{2+} sparks. This is extremely important regarding the amount of Ca^{2+} stored in the SR, as the RyR is also sensitive to luminal Ca^{2+} and below a certain threshold, Ca^{2+} sparks are shut down (Zima et al., 2010). Thus, in the setting of decreased SR Ca^{2+} load or depressed levels of ATP, as in HF, spontaneous Ca^{2+} sparks can be depressed. In permeabilized myocytes, we avoid this by controlling the intracellular solution. Using this maneuver, we unmasked the enhanced RyR activity in PMI myocytes, showing a marked increase in the Ca^{2+} spark frequency (Fig. 3). Under these conditions, the SR Ca^{2+} load was not significantly different from sham and PMI cells (Fig. 5 A), indicating that SR Ca^{2+} depletion in HF contributes to the depressed Ca^{2+} spark occurrence in PMI mice cardiomyocytes, but this may not be a unique mechanism. In fact, HF is a highly compromised metabolic state where substances that influence RyR activity, like ATP concentration, are altered (Meissner et al., 1986; Ingwall, 2006, 2009; Laver, 2010; Tencerová et al., 2012). In fact, in a subset of experiments, we tested the effect on Ca^{2+} sparks of a metabolically altered intracellular solution (similar to what could be found in HF; see Materials and methods) in the same cardiomyocyte by perfusing first with the basic control solution and then with the failing solution (Fig. 6 A). The results unequivocally show that the "failing" solution drastically reduces Ca^{2+} spark occurrence, even in the cells isolated from PMI mice, where the Ca^{2+} spark frequency was enhanced, demonstrating that the intracellular environment around the RyR can contribute to mask the otherwise enhanced Ca^{2+} spark frequency. Moreover, the effects of luminal Ca^{2+} on RyR modulation by ATP are synergistic (Tencerová et al., 2012). But once the Ca^{2+} spark happens (stochastically and/or under β-adrenergic stimulation, which also increases SR load), the probability of this Ca^{2+} spark initiating a Ca^{2+} wave is higher in PMI cells, likely because of RyR hyperactivity and SERCA depression. The differences in Ca^{2+} spark properties between sham and PMI cells were maintained in every condition tested, suggesting alterations in the RyR gating and/or rearrangement of clusters.

Thus, our data show that although the RyR is more active and may induce more leak in HF, this may occur preferably in nonspark form. However, the enhanced sensitivity to Ca^{2+} of the RyR in HF may favor propagation of Ca^{2+} sparks into Ca^{2+} waves, which contrary to Ca^{2+} sparks, are arrhythmogenic by activating NCX current.

We are grateful to the ANIMEX platform for animal care, Renée Ventura-Clapier for discussions about intracellular metabolic alterations in HF, and Françoise Boussac for secretarial assistance.

This study was supported by grants from Agence Nationale de la Recherche (ANR-13-BSV1-0023-01), Fondation pour la Recherche Medicale (program cardiovasculaire 2011), Fundación Mutua Madrileña and Fundación Eugenio Rodriguez Pascual (to G. Ruiz-Hurtado). G. Ruiz-Hurtado was funded by a Servier contract and by the Ministerio de Economía y Competitividad in the Juan de la Cierva postdoctoral program from Spain.

The authors declare no competing financial interests.

Author contributions: G. Ruiz-Hurtado and L. Li did most of the collection, analysis, and interpretation of data. A. Rueda, M. Fernández-Velasco and Y.Y. Wang participated in collection, analysis, and interpretation. C. Cassan, B. Gellen, and F. Lefebvre performed the animal surgery. C. Cassan and P. Mateo recorded and analyzed echocardiograms. J.-P. Benitah and A.M. Gomez did the conception, design of the experiments, and some analyses. G. Ruiz-Hurtado and A.M. Gomez did the first drafting of the article, and all other authors revised it critically for important intellectual content. All authors approved the final version of the manuscript. All persons designated as authors qualify for authorship, and all those who qualify for authorship are listed.

Eduardo Rios served as editor.

Submitted: 18 January 2015
Accepted: 19 August 2015

REFERENCES

Ai, X., J.W. Curran, T.R. Shannon, D.M. Bers, and S.M. Pogwizd. 2005. Ca^{2+}/calmodulin-dependent protein kinase modulates cardiac ryanodine receptor phosphorylation and sarcoplasmic reticulum Ca^{2+} leak in heart failure. *Circ. Res.* 97:1314–1322. http://dx.doi.org/10.1161/01.RES.0000194329.41863.89

Belevych, A.E., D. Terentyev, R. Terentyeva, Y. Nishijima, A. Sridhar, R.L. Hamlin, C.A. Carnes, and S. Györke. 2011. The relationship between arrhythmogenesis and impaired contractility in heart failure: role of altered ryanodine receptor function. *Cardiovasc. Res.* 90:493–502. http://dx.doi.org/10.1093/cvr/cvr025

Bénitah, J.P., B.G. Kerfant, G. Vassort, S. Richard, and A.M. Gómez. 2002. Altered communication between L-type calcium channels and ryanodine receptors in heart failure. *Front. Biosci.* 7:e263–e275. http://dx.doi.org/10.2741/benitah

Bers, D.M. 2002. Cardiac excitation-contraction coupling. *Nature.* 415:198–205. http://dx.doi.org/10.1038/415198a

Beuckelmann, D.J., M. Näbauer, and E. Erdmann. 1992. Intracellular calcium handling in isolated ventricular myocytes from patients with terminal heart failure. *Circulation.* 85:1046–1055. http://dx.doi.org/10.1161/01.CIR.85.3.1046

Cheng, H., W.J. Lederer, and M.B. Cannell. 1993. Calcium sparks: elementary events underlying excitation-contraction coupling in heart muscle. *Science.* 262:740–744. http://dx.doi.org/10.1126/science.8235594

Dahlöf, B. 2010. Cardiovascular disease risk factors: Epidemiology and risk assessment. *Am. J. Cardiol.* 105:3A–9A. http://dx.doi.org/10.1016/j.amjcard.2009.10.007

Fabiato, A., and F. Fabiato. 1975. Contractions induced by a calcium-triggered release of calcium from the sarcoplasmic reticulum of single skinned cardiac cells. *J. Physiol.* 249:469–495. http://dx.doi.org/10.1113/jphysiol.1975.sp011026

Fernández-Velasco, M., A. Rueda, N. Rizzi, J.P. Benitah, B. Colombi, C. Napolitano, S.G. Priori, S. Richard, and A.M. Gómez. 2009. Increased Ca^{2+} sensitivity of the ryanodine receptor mutant RyR2R4496C underlies catecholaminergic polymorphic ventricular tachycardia. *Circ. Res.* 104:201–209. http://dx.doi.org/10.1161/CIRCRESAHA.108.177493

Fernández-Velasco, M., G. Ruiz-Hurtado, A. Rueda, P. Neco, M. Mercado-Morales, C. Delgado, C. Napolitano, S.G. Priori, S. Richard, A.M. Gómez, and J.P. Benitah. 2011. $RyRCa^{2+}$ leak limits cardiac Ca^{2+} window current overcoming the tonic effect of calmodulinin mice. *PLoS ONE.* 6:e20863. http://dx.doi.org/10.1371/journal.pone.0020863

Fischer, T.H., J. Herting, T. Tirilomis, A. Renner, S. Neef, K. Toischer, D. Ellenberger, A. Förster, J.D. Schmitto, J. Gummert, et al. 2013. Ca^{2+}/calmodulin-dependent protein kinase II and protein kinase A differentially regulate sarcoplasmic reticulum Ca^{2+} leak in human cardiac pathology. *Circulation.* 128:970–981. http://dx.doi.org/10.1161/CIRCULATIONAHA.113.001746

Gaughan, J.P., S. Furukawa, V. Jeevanandam, C.A. Hefner, H. Kubo, K.B. Margulies, B.S. McGowan, J.A. Mattiello, K. Dipla, V. Piacentino III, et al. 1999. Sodium/calcium exchange contributes to contraction and relaxation in failed human ventricular myocytes. *Am. J. Physiol.* 277:H714–H724.

Gómez, A.M., H.H. Valdivia, H. Cheng, M.R. Lederer, L.F. Santana, M.B. Cannell, S.A. McCune, R.A. Altschuld, and W.J. Lederer. 1997. Defective excitation-contraction coupling in experimental cardiac hypertrophy and heart failure. *Science.* 276:800–806. http://dx.doi.org/10.1126/science.276.5313.800

Gómez, A.M., S. Guatimosim, K.W. Dilly, G. Vassort, and W.J. Lederer. 2001. Heart failure after myocardial infarction: Altered excitation-contraction coupling. *Circulation.* 104:688–693. http://dx.doi.org/10.1161/hc3201.092285

Gómez, A.M., B. Schwaller, H. Porzig, G. Vassort, E. Niggli, and M. Egger. 2002. Increased exchange current but normal Ca^{2+} transport via Na^{+}-Ca^{2+} exchange during cardiac hypertrophy after myocardial infarction. *Circ. Res.* 91:323–330. http://dx.doi.org/10.1161/01.RES.0000031384.55006.DB

Györke, S., and D. Terentyev. 2008. Modulation of ryanodine receptor by luminal calcium and accessory proteins in health and cardiac disease. *Cardiovasc. Res.* 77:245–255. http://dx.doi.org/10.1093/cvr/cvm038

Ingwall, J.S. 2006. On the hypothesis that the failing heart is energy starved: Lessons learned from the metabolism of ATP and creatine. *Curr. Hypertens. Rep.* 8:457–464. http://dx.doi.org/10.1007/s11906-006-0023-x

Ingwall, J.S. 2009. Energy metabolism in heart failure and remodelling. *Cardiovasc. Res.* 81:412–419. http://dx.doi.org/10.1093/cvr/cvn301

Kubo, H., K.B. Margulies, V. Piacentino III, J.P. Gaughan, and S.R. Houser. 2001. Patients with end-stage congestive heart failure treated with beta-adrenergic receptor antagonists have improved ventricular myocyte calcium regulatory protein abundance. *Circulation.* 104:1012–1018. http://dx.doi.org/10.1161/hc3401.095073

Laver, D.R. 2006. Regulation of ryanodine receptors from skeletal and cardiac muscle during rest and excitation. *Clin. Exp. Pharmacol. Physiol.* 33:1107–1113. http://dx.doi.org/10.1111/j.1440-1681.2006.04500.x

Laver, D.R. 2010. Regulation of RyR channel gating by Ca^{2+}, Mg^{2+} and ATP. *Curr Top Membr.* 66:69–89. http://dx.doi.org/10.1016/S1063-5823(10)66004-8

Lindner, M., M.C. Brandt, H. Sauer, J. Hescheler, T. Böhle, and D.J. Beuckelmann. 2002. Calcium sparks in human ventricular cardiomyocytes from patients with terminal heart failure. *Cell Calcium.* 31:175–182. http://dx.doi.org/10.1054/ceca.2002.0272

Lipp, P., and E. Niggli. 1996. Submicroscopic calcium signals as fundamental events of excitation–contraction coupling in guinea-pig cardiac myocytes. *J. Physiol.* 492:31–38. http://dx.doi.org/10.1113/jphysiol.1996.sp021286

Lloyd-Jones, D.M. 2010. Cardiovascular risk prediction: Basic concepts, current status, and future directions. *Circulation.* 121:1768–1777. http://dx.doi.org/10.1161/CIRCULATIONAHA.109.849166

Marx, S.O., S. Reiken, Y. Hisamatsu, T. Jayaraman, D. Burkhoff, N. Rosemblit, and A.R. Marks. 2000. PKA phosphorylation dissociates FKBP12.6 from the calcium release channel (ryanodine receptor): Defective regulation in failing hearts. *Cell.* 101:365–376. http://dx.doi.org/10.1016/S0092-8674(00)80847-8

Meissner, G., E. Darling, and J. Eveleth. 1986. Kinetics of rapid calcium release by sarcoplasmic reticulum. Effects of calcium, magnesium, and adenine nucleotides. *Biochemistry.* 25:236–244. http://dx.doi.org/10.1021/bi00349a033

Mercadier, J.J., A.M. Lompré, P. Duc, K.R. Boheler, J.B. Fraysse, C. Wisnewsky, P.D. Allen, M. Komajda, and K. Schwartz. 1990. Altered sarcoplasmic reticulum Ca^{2+}-ATPase gene expression in the human ventricle during end-stage heart failure. *J. Clin. Invest.* 85:305–309. http://dx.doi.org/10.1172/JCI114429

Meyer, M., W. Schillinger, B. Pieske, C. Holubarsch, C. Heilmann, H. Posival, G. Kuwajima, K. Mikoshiba, H. Just, G. Hasenfuss, et al. 1995. Alterations of sarcoplasmic reticulum proteins in failing human dilated cardiomyopathy. *Circulation.* 92:778–784. http://dx.doi.org/10.1161/01.CIR.92.4.778

Milliez, P., S. Messaoudi, J. Nehme, C. Rodriguez, J.L. Samuel, and C. Delcayre. 2009. Beneficial effects of delayed ivabradine treatment on cardiac anatomical and electrical remodeling in rat severe chronic heart failure. *Am. J. Physiol. Heart Circ. Physiol.* 296:H435–H441. http://dx.doi.org/10.1152/ajpheart.00591.2008

Neubauer, S. 2007. The failing heart—an engine out of fuel. *N. Engl. J. Med.* 356:1140–1151. http://dx.doi.org/10.1056/NEJMra063052

Pereira, L., J. Matthes, I. Schuster, H.H. Valdivia, S. Herzig, S. Richard, and A.M. Gómez. 2006. Mechanisms of $[Ca^{2+}]_i$ transient decrease in cardiomyopathy of *db/db* type 2 diabetic mice. *Diabetes.* 55:608–615. http://dx.doi.org/10.2337/diabetes.55.03.06.db05-1284

Pereira, L., G. Ruiz-Hurtado, E. Morel, A.C. Laurent, M. Métrich, A. Domínguez-Rodríguez, S. Lauton-Santos, A. Lucas, J.P. Benitah, D.M. Bers, et al. 2012. Epac enhances excitation–transcription coupling in cardiac myocytes. *J. Mol. Cell. Cardiol.* 52:283–291. http://dx.doi.org/10.1016/j.yjmcc.2011.10.016

Perrier, E., B.G. Kerfant, N. Lalevee, P. Bideaux, M.F. Rossier, S. Richard, A.M. Gómez, and J.P. Benitah. 2004. Mineralocorticoid receptor antagonism prevents the electrical remodeling that precedes cellular hypertrophy after myocardial infarction. *Circulation.* 110:776–783. http://dx.doi.org/10.1161/01.CIR.0000138973.55605.38

Piacentino, V., III, C.R. Weber, X. Chen, J. Weisser-Thomas, K.B. Margulies, D.M. Bers, and S.R. Houser. 2003. Cellular basis of abnormal calcium transients of failing human ventricular myocytes. *Circ. Res.* 92:651–658. http://dx.doi.org/10.1161/01.RES.0000062469.83985.9B

Reiken, S., M. Gaburjakova, S. Guatimosim, A.M. Gómez, J. D'Armiento, D. Burkhoff, J. Wang, G. Vassort, W.J. Lederer, and A.R. Marks. 2003. Protein kinase A phosphorylation of the cardiac calcium release channel (ryanodine receptor) in normal and failing hearts. Role of phosphatases and response to isoproterenol. *J. Biol. Chem.* 278:444–453. http://dx.doi.org/10.1074/jbc.M207028200

Ruiz-Hurtado, G., M. Fernández-Velasco, M. Mourelle, and C. Delgado. 2007. LA419, a novel nitric oxide donor, prevents pathological cardiac remodeling in pressure-overloaded rats via endothelial nitric oxide synthase pathway regulation. *Hypertension.* 50:1049–1056. http://dx.doi.org/10.1161/HYPERTENSIONAHA.107.093666

Ruiz-Hurtado, G., A. Domínguez-Rodríguez, L. Pereira, M. Fernández-Velasco, C. Cassan, F. Lezoualc'h, J.P. Benitah, and A.M. Gómez. 2012a. Sustained Epac activation induces calmodulin dependent positive inotropic effect in adult cardiomyocytes. *J. Mol. Cell. Cardiol.* 53:617–625. http://dx.doi.org/10.1016/j.yjmcc.2012.08.004

Ruiz-Hurtado, G., N. Gómez-Hurtado, M. Fernández-Velasco, E. Calderón, T. Smani, A. Ordoñez, V. Cachofeiro, L. Boscá, J. Díez, A.M. Gómez, and C. Delgado. 2012b. Cardiotrophin-1 induces sarcoplasmic reticulum Ca^{2+} leak and arrhythmogenesis in adult rat ventricular myocytes. *Cardiovasc. Res.* 96:81–89. http://dx.doi.org/10.1093/cvr/cvs234

Shorofsky, S.R., R. Aggarwal, M. Corretti, J.M. Baffa, J.M. Strum, B.A. Al-Seikhan, Y.M. Kobayashi, L.R. Jones, W.G. Wier, and C.W. Balke. 1999. Cellular mechanisms of altered contractility in the hypertrophied heart: Big hearts, big sparks. *Circ. Res.* 84:424–434. http://dx.doi.org/10.1161/01.RES.84.4.424

Tencerová, B., A. Zahradníková, J. Gaburjáková, and M. Gaburjáková. 2012. Luminal Ca^{2+} controls activation of the cardiac ryanodine receptor by ATP. *J. Gen. Physiol.* 140:93–108. http://dx.doi.org/10.1085/jgp.201110708

Terentyev, D., I. Györke, A.E. Belevych, R. Terentyeva, A. Sridhar, Y. Nishijima, E.C. de Blanco, S. Khanna, C.K. Sen, A.J. Cardounel, et al. 2008. Redox modification of ryanodine receptors contributes to sarcoplasmic reticulum Ca^{2+} leak in chronic heart failure. *Circ. Res.* 103:1466–1472. http://dx.doi.org/10.1161/CIRCRESAHA.108.184457

Trafford, A.W., M.E. Díaz, and D.A. Eisner. 1998. Measurement of sarcoplasmic reticulum Ca content and sarcolemmal fluxes during the transient stimulation of the systolic Ca transient produced by caffeine. *Ann. NY Acad. Sci.* 853:368–371. http://dx.doi.org/10.1111/j.1749-6632.1998.tb08302.x

Wagner, E., M.A. Lauterbach, T. Kohl, V. Westphal, G.S. Williams, J.H. Steinbrecher, J.H. Streich, B. Korff, H.T. Tuan, B. Hagen, et al. 2012. Stimulated emission depletion live-cell super-resolution imaging shows proliferative remodeling of T-tubule membrane structures after myocardial infarction. *Circ. Res.* 111:402–414. http://dx.doi.org/10.1161/CIRCRESAHA.112.274530

Zima, A.V., E. Bovo, D.M. Bers, and L.A. Blatter. 2010. Ca^{2+} spark-dependent and -independent sarcoplasmic reticulum Ca^{2+} leak in normal and failing rabbit ventricular myocytes. *J. Physiol.* 588:4743–4757. http://dx.doi.org/10.1113/jphysiol.2010.197913